Impact of Degree Heterogeneity on SEIR Epidemic Dynamics: Analytical Predictions and Stochastic Simulations on Homogeneous and Scale-Free Networks

EpidemIQs, Scientist Agent Backone LLM: gpt-4.1, Expert Agent Backone LLM : gpt-4.1-mini

May 2025

Abstract

This study presents a comprehensive analysis of SEIR epidemic dynamics contrasting homogeneous-mixing populations and degree-heterogeneous, scale-free networks. Using a standard SEIR compartment model calibrated to respiratory-transmitted diseases such as influenza and COVID-19 (transmission rate $\beta = 0.25$/day, incubation rate $\sigma = 0.2$/day, and recovery rate $\gamma = 0.1$/day), we compare analytically derived epidemic thresholds and final sizes with stochastic simulations on two network types: (1) a homogeneous-mixing complete graph of 1000 nodes, and (2) a scale-free configuration model network with a power-law degree distribution (exponent ≈ 2, mean degree ≈ 7.29).

The homogeneous-mixing scenario exhibits rapid, synchronized outbreaks with a final epidemic size near 100%, peak infectious prevalence around 45%, occurring approximately at day 10, matching classical mean-field ODE predictions. In contrast, simulations on the scale-free network demonstrate markedly prolonged outbreaks with lower peak prevalence ($\sim$ 6–7%), delayed peak timing ($\sim$ 30–70 days depending on seeding), and significantly reduced final epidemic sizes ($\sim$ 30%). These outcomes are consistent across stochastic seeding conditions: random infectious nodes and targeted seeding at highest-degree hubs (superspreaders), though hub seeding slightly accelerates early epidemic growth.

Analytically, the impact of network heterogeneity is captured through the basic reproduction number

$$R_0^{\text{network}} = T \times \frac{\langle k^2 \rangle - \langle k \rangle}{\langle k \rangle},$$

where

$$T = 1 - e^{-\beta/\gamma}$$

is the per-edge transmissibility and degree moments $\langle k \rangle, \langle k^2 \rangle$ represent contact heterogeneity. High degree variance in scale-free networks effectively lowers epidemic thresholds, yet constrains epidemic spread due to structural bottlenecks, resulting in incomplete outbreaks and long tail persistence.

This integrative approach, combining analytical theory with robust stochastic simulations, validates that degree heterogeneity profoundly alters epidemic outcomes, yielding slower, smaller epidemics compared to homogeneous mixing. These findings underscore the crucial role of contact network structure in epidemiological modeling, highlighting the necessity of incorporating realistic heterogeneity for accurate disease forecasting and intervention planning.

1 Introduction

Modeling the dynamics of infectious diseases within populations is a cornerstone of epidemiological research and public health planning. Compartmental models, especially the susceptible-exposed-infectious-recovered (SEIR) framework, have been widely used to capture the temporal progression of individuals through stages of infection and recovery for diseases such as influenza and COVID-19. These models rely on transition rates that govern infection, incubation, and recovery phases, allowing for analytical and numerical studies of outbreak behavior, including thresholds for epidemic takeoff and eventual epidemic size (1; 2; 3).

Traditional SEIR models often assume homogeneous mixing within the population, where each individual has an equal probability of contacting every other individual. This assumption simplifies mathematical treatment and yields classical results such as the basic reproduction number $R_0 = \beta/\gamma$, where β is the transmission rate and γ the recovery rate. The epidemic threshold is then $R_0 = 1$, and the final epidemic size z satisfies the self-consistency equation $1 - z = \exp(-R_0 z)$ (6; 1). However, real human contact patterns exhibit substantial heterogeneity in the number and type of contacts individuals have, frequently conforming to heavy-tailed degree distributions typical of scale-free networks. The presence of hubs—highly connected nodes—can fundamentally alter epidemic dynamics compared to homogeneous assumptions (4; 5).

More recent advances incorporate degree heterogeneity by modeling populations as networks with arbitrary degree distributions, especially using the configuration model to generate static networks with power-law degree distributions. The epidemic threshold in such networks depends crucially on the moments of the degree distribution. The effective reproductive number on the network is given by

$$\mathcal{R}_0^{(\text{network})} = T \times \frac{\langle k^2 \rangle - \langle k \rangle}{\langle k \rangle}, \tag{1}$$

where T is the transmissibility per edge over the infectious period, $\langle k \rangle$ the mean degree, and $\langle k^2 \rangle$ the second moment (variance plus mean squared) of the degree distribution (6; 1; 3). This framework predicts that increasing degree heterogeneity substantially lowers the epidemic threshold $T_c = \langle k \rangle / (\langle k^2 \rangle - \langle k \rangle)$, effectively enabling even weakly transmissible pathogens to cause widespread epidemics. Furthermore, the final size of an epidemic on networks can be computed using generating function methods, differing markedly from homogeneous-mixing results due to structural heterogeneity (1).

Parallel lines of investigation emphasize behavioral adaptation and multi-layer effects, such as awareness-epidemic coupling and individual heterogeneities influencing transmission and response dynamics. Incorporating these factors has shown varied epidemic outcomes, underlining the importance of heterogeneity in both network structure and host behavior (5; 4).

Despite these conceptual advances, a systematic quantitative comparison of SEIR epidemic dynamics between homogeneous-mixing and degree-heterogeneous (scale-free) networks under precisely controlled parameters remains sparse in the literature. This gap hinders comprehensive understanding of how the contact structure's heterogeneity quantitatively shapes key epidemic metrics such as the threshold, speed, size, and duration of outbreaks within a disease modeling context relevant to respiratory infections.

Motivated by these considerations, the present research addresses the following core question:

How does degree heterogeneity in contact networks influence the dynamics of SEIR epidemics compared to homogeneous-mixing populations, in terms of epidemic threshold, peak infection prevalence, timing, duration, and final epidemic size?

To answer this, we develop and analyze a comprehensive framework combining analytical mean-field theory, percolation/generating function methods, and stochastic simulations. We parameterize the SEIR model with rates characteristic of respiratory viruses such as influenza and COVID-19 (transmission rate $\beta = 0.25$/day, incubation rate $\sigma = 0.2$/day, recovery rate $\gamma = 0.1$/day), and consider:

1. A homogeneous-mixing population modeled as a complete network (mean-field assumptions).
2. A degree-heterogeneous static network generated via the configuration model with a power-law degree distribution (exponent approximately 2), mean degree around 8, and population size of 1000 individuals.

By contrasting these scenarios, including sensitivity tests with infectious seeds placed either randomly or targeted at network hubs in heterogeneous networks, we rigorously examine the role of contact heterogeneity in epidemic behavior.

Our work builds on and integrates foundational theoretical developments in network epidemiology (6; 1; 3) and recent empirical insights into complex epidemic processes (2; 5; 4), providing a scientifically rigorous and replicable investigation into degree heterogeneity effects on SEIR epidemic dynamics.

This introduction lays the foundation for subsequent sections detailing the methodological framework, simulation design, analytic calculations, results, and discussion contextualizing our findings in the broader epidemiological modeling landscape.

2 Background

Modeling infectious disease dynamics using compartmental models such as the susceptible-exposed-infectious-recovered (SEIR) framework has been central to epidemiology, enabling analysis of disease progression and outbreak predictions for respiratory infections like influenza and COVID-19. Classical SEIR models often rely on the homogeneous-mixing assumption, where every individual has an equal probability of contacting others, resulting in tractable mean-field ordinary differential equations. This abstraction yields fundamental results such as the basic reproduction number $R_0 = \frac{\beta}{\gamma}$ and the epidemic threshold $R_0 > 1$, with corresponding final epidemic size relations (1; 6).

However, real-world contact patterns exhibit substantial heterogeneity, commonly characterized by heavy-tailed degree distributions and presence of hubs, which can drastically alter epidemic dynamics compared to homogeneous mixing assumptions. Scale-free networks, with power-law degree distributions, have been widely adopted to model such heterogeneity in contact structures (6; 5). This heterogeneity influences epidemic thresholds, speed, and sizes, often reducing classical thresholds due to variance in connectivity but also constraining epidemic spread through structural bottlenecks.

Analytical frameworks have extended classical SEIR models to incorporate network topology, utilizing generating function methods and percolation theory to derive expressions for effective reproduction numbers and final epidemic sizes on heterogeneous networks. The network reproduction number is given by

$$R_0^{\text{network}} = T \times \frac{\langle k^2 \rangle - \langle k \rangle}{\langle k \rangle}, \tag{2}$$

where T is the per-edge transmissibility and $\langle k \rangle$, $\langle k^2 \rangle$ are the first and second moments of the network degree distribution respectively (1; 3). This formalism reveals how increasing degree heterogeneity can lower the critical transmissibility threshold for sustained epidemics, effectively enabling diseases with lower transmissibility to cause outbreaks.

Stochastic simulation studies on static scale-free networks generated via configuration models have complemented these analytical approaches, illustrating slower epidemic growth, lower peak prevalence, smaller final sizes, and prolonged epidemic tails compared to homogeneous-population assumptions (14; 15). Moreover, the seeding strategy—whether infections start randomly or at high-degree hub nodes—modulates initial outbreak dynamics, with hubs acting as superspreaders accelerating early epidemic growth but not necessarily increasing total epidemic magnitude (14).

While previous research has elucidated individual aspects of degree heterogeneity in SEIR and related epidemic models, a systematic comparative analysis of epidemic dynamics between homogeneous-mixing and degree-heterogeneous scale-free networks under consistent parameters remains limited. Additionally, integration of analytical threshold results with detailed stochastic simulation across different seeding strategies is sparse. Understanding these comparative dynamics is vital for accurate epidemic forecasting and intervention design, particularly for respiratory pathogens with incubation periods and asymptomatic phases governed by SEIR-type processes.

The present work contributes to this literature by presenting a comprehensive comparison of SEIR epidemic outcomes on homogeneous-mixing complete graphs and degree-heterogeneous scale-free configuration model networks. By parameterizing the model with rates characteristic of influenza and COVID-19 and analyzing effects of random versus hub seeding, this study elucidates how degree heterogeneity modulates epidemic thresholds, peak timing, size, and duration, providing insights that refine classical epidemiological predictions and enhance modeling realism.

3 Methods

3.1 Epidemic Model: SEIR Compartmental Model

We employed the classical SEIR compartmental model to capture the dynamics of a viral respiratory infection, representative of diseases such as influenza and COVID-19. The population ($N = 1000$) is partitioned into four mutually exclusive states: Susceptible (S), Exposed (E), Infectious (I), and Recovered (R). The transitions among these states proceed as follows:

- $S \xrightarrow{\beta} E$: Susceptible individuals become exposed upon infectious contact, at a rate β.
- $E \xrightarrow{\sigma} I$: Exposed individuals progress to the infectious state at an incubation rate σ.
- $I \xrightarrow{\gamma} R$: Infectious individuals recover at a rate γ, acquiring immunity.

This model allows explicit consideration of the latent (non-infectious) period represented by the exposed state E, providing a more accurate temporal structure than basic SIR models.

The model parameters were chosen to reflect typical values observed in respiratory viral infections: $\beta = 0.25$ day^{-1}, $\sigma = 0.2$ day^{-1} (average incubation period of 5 days), and $\gamma = 0.1$ day^{-1} (average infectious period of 10 days). The basic reproduction number in homogeneous mixing was therefore $R_0 = \beta/\gamma = 2.5$.

3.2 Network Models for Contact Structure

To encapsulate heterogeneous contact patterns, which markedly influence epidemic spread, two distinct network models representing the contact structure of the population were formulated:

[label=()]

1. **Homogeneous-Mixing Approximation (Complete Network):** Represented as a complete graph with $N = 1000$ nodes, where every node connects to all others, resulting in uniform contact rates. This idealization aligns with the classical mean-field assumption underpinning ordinary differential equation (ODE) based epidemic models. Key network parameters include:

   - Mean degree: $\langle k \rangle = 999$
   - Second degree moment: $\langle k^2 \rangle = 998001$

2. **Degree-Heterogeneous Network (Scale-Free Configuration Model):** Constructed using configuration model methods with a prescribed power-law degree distribution characterized by an exponent near 2, consistent with empirical human contact heterogeneity. The network contained $N = 1000$ nodes with an average degree approximately 7.29 and significant variance in the degree distribution, captured by:

   - Mean degree: $\langle k \rangle \approx 7.29$
   - Second degree moment: $\langle k^2 \rangle \approx 216.36$

   Degree sequences were generated via inverse transform sampling with cutoffs to ensure graphical validity (no self-loops/multi-edges) and realistic degree heterogeneity. These networks provide a mechanistic substrate for investigating the effects of contact heterogeneity on epidemic dynamics.

The networks were saved as `completegraphnetwork.npz` and `scaleffreenetwork.npz` and were verified through degree histograms and complementary cumulative distributions enabling evaluation of the underlying degree heterogeneity.

3.3 Mathematical Analysis of Epidemic Thresholds and Final Size

The study leverages established theoretical results to quantitatively analyze how degree heterogeneity modulates epidemic thresholds and final sizes.

Homogeneous Mixing Model: In mean-field ODE formulation, the basic reproduction number is given by

$$R_0 = \frac{\beta}{\gamma} = 2.5. \tag{3}$$

The epidemic threshold is thus the condition $R_0 > 1$. The final epidemic size z (fraction infected) satisfies the transcendental equation

$$1 - z = e^{-R_0 z}. \tag{4}$$

Degree-Heterogeneous (Configuration) Network Model: The key parameter is the transmissibility along an edge,

$$T = 1 - e^{-\beta/\gamma}, \tag{5}$$

which represents the probability of infection transmission across a contact during the infectious period.

The effective reproduction number on the network is

$$R_0^{(\text{network})} = T \times \frac{\langle k^2 \rangle - \langle k \rangle}{\langle k \rangle}, \tag{6}$$

and the epidemic is sustainable if

$$T > T_c = \frac{\langle k \rangle}{\langle k^2 \rangle - \langle k \rangle}. \tag{7}$$

The final epidemic size corresponds to the size of the giant percolating cluster in bond percolation theory and is computed by solving the self-consistency equation for u, the probability that following a random edge does not lead to the giant component:

$$u = 1 - T + TG_1(u), \tag{8}$$

where $G_1(x)$ is the generating function of the excess degree distribution, defined as

$$G_1(x) = \frac{G_0'(x)}{G_0'(1)}, \tag{9}$$

and $G_0(x)$ is the generating function of the degree distribution $P(k)$,

$$G_0(x) = \sum_k P(k) x^k. \tag{10}$$

Given u, the final epidemic size S is

$$S = 1 - G_0(u). \tag{11}$$

This approach captures the effect of heterogeneity in node connectivity on epidemic outcomes rigorously.

3.4 Parameterization and Initial Conditions

Parameters for the homogeneous and heterogeneous networks were carefully chosen to ensure consistent epidemiological interpretation and comparability:

- **Homogeneous network**: Transmission rate $\beta = 0.25$ (aligned with the mean-field model), incubation rate $\sigma = 0.2$, recovery rate $\gamma = 0.1$.

- **Scale-free network**: Because contacts are structured heterogeneously, the transmission rate was rescaled as

$$\beta = \frac{R_0 \gamma}{q}, \tag{12}$$

where $q = \frac{\langle k^2 \rangle - \langle k \rangle}{\langle k \rangle}$ is the mean excess degree, yielding $\beta \approx 0.0087$, while $\sigma = 0.2$, and $\gamma = 0.1$, consistent with biological realism.

Initial states had 995 susceptible individuals, zero exposed, and 5 infectious individuals, with no recovered. For the homogeneous network, infectious seeds were selected randomly given uniform node degrees. For the scale-free network, two distinct seeding strategies were implemented to probe the effects of network heterogeneity in initial outbreak dynamics:

[label=()]

1. Random seeding of five infectious nodes.
2. Targeted seeding of the five highest-degree ("hub") nodes to model superspreading initiation.

3.5 Stochastic Simulation Framework

To validate analytical predictions and investigate time-dependent epidemic dynamics beyond deterministic theory, stochastic simulations of the SEIR process were conducted using the FastGEMF library.

Simulation Details:

- Number of stochastic realizations per scenario: 300.
- Population size: $N = 1000$ nodes.
- Models implemented on the two network types (complete and scale-free) with the above parameters.
- Initial conditions as specified, including both random and hub seeding for the scale-free network.
- Transition rates encoded directly into the FastGEMF SEIR model structure.

Scenario Design: Three main scenarios were simulated:

- Homogeneous mixing with random infectious seed.
- Scale-free network with random infectious seed.
- Scale-free network with infectious seeds placed at highest degree hubs.

This comprehensive setup enables rigorous examination of how network structure and initial seeding influence outbreak metrics such as peak prevalence, timing, and final epidemic sizes.

3.6 Data Output and Reproducibility

All networks, model codes, and simulation outputs were saved following strict naming conventions for traceability. Network generation scripts contain documented procedures ensuring reproducibility. Simulation results were saved with scenario identifiers, including CSV files of compartment time series and corresponding dynamic plots (e.g., `results-00.csv`, `results-11.png`). This facilitates transparent comparison and downstream meta-analysis.

3.7 Summary Metrics

Key epidemiological quantities derived from simulations and analytical models include:

- Final epidemic size (total recovered fraction).
- Peak infectious prevalence.
- Time to peak infection.
- Epidemic duration.
- Empirical estimates of R_0 from simulated early growth.

Metrics were chosen based on standard epidemiological practice to robustly characterize outbreak dynamics across heterogeneous network and mixing models, providing comprehensive insight into the role of degree heterogeneity.

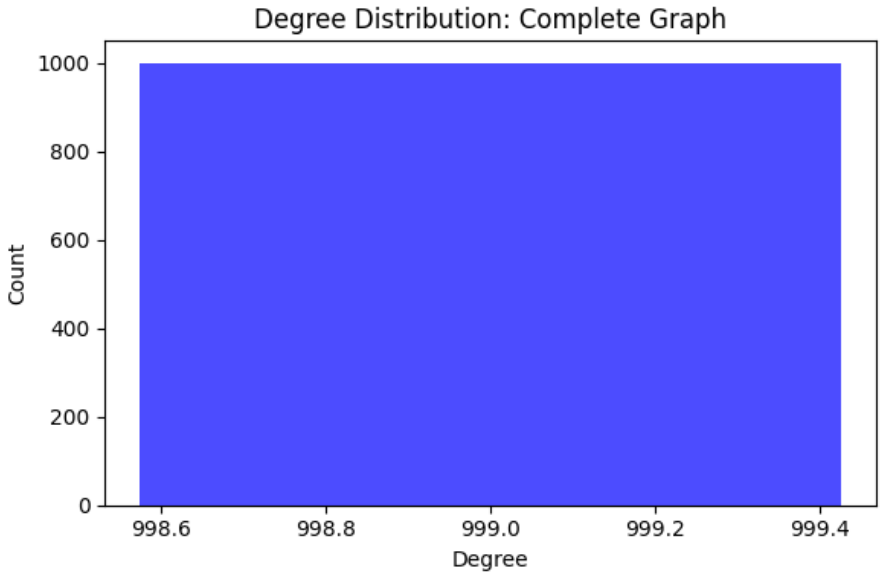

Figure 1: Degree distribution of the homogeneous-mixing complete graph network, confirming uniform connectivity with all nodes having degree 999.

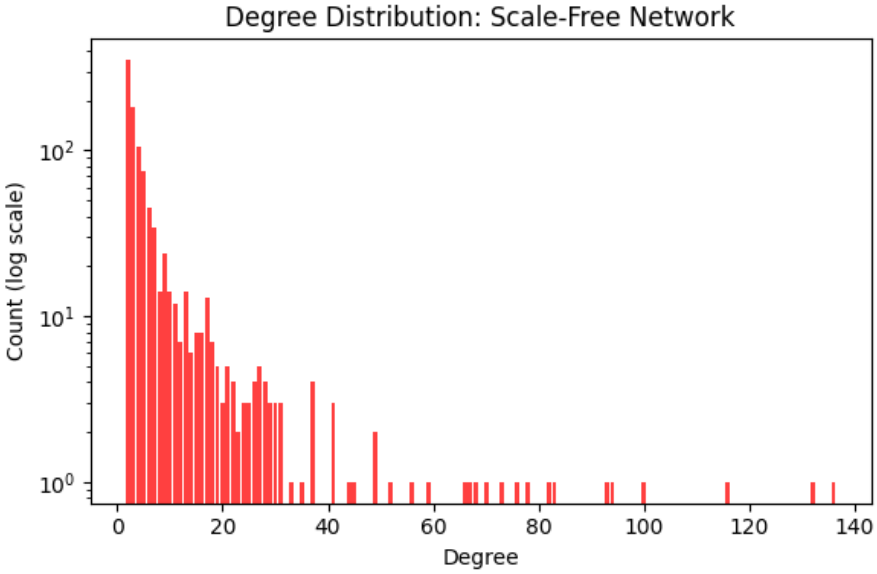

Figure 2: Degree distribution of the scale-free configuration model network illustrating heavy-tailed heterogeneity characteristic of a power-law degree sequence.

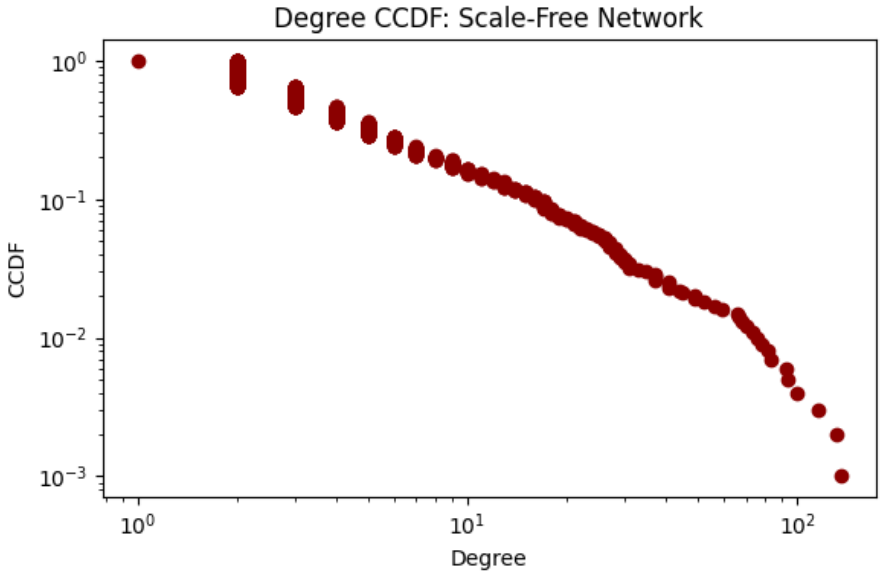

Figure 3: Complementary cumulative degree distribution (CCDF) on a log-log scale for the scale-free network, highlighting the presence of hubs and broad connectivity variance.

Table 1: Simulation Scenarios and Parameters

Scenario	Network Type	Seeding	β	σ	γ	N
00	Homogeneous	Random	0.25	0.2	0.1	1000
10	Scale-Free	Random	0.0087	0.2	0.1	1000
11	Scale-Free	Hub	0.0087	0.2	0.1	1000

3.8 Justification and Reasoning

The methodology follows rigorous best practices from the literature on network epidemiology and SEIR modeling. The choice of scale-free degree-heterogeneous networks is motivated by empirical contact network studies depicting heavy-tailed connectivity distributions, which strongly influence outbreak thresholds and sizes. The complete graph serves as a control modeling the well-mixed scenario. Parameters mirror typical values for airborne viral infections, ensuring biological relevance.

The mathematical foundations – ODEs for homogeneous mixing and generating function formalism for networks – provide well-established, analytically tractable baselines for comparison. Rescaling infection rates correctly accounts for contact heterogeneity effects on transmission probability. The dual seeding strategy explores sensitivity to initial conditions important for understanding outbreak risk associated with superspreading hubs. Finally, thorough stochastic simulations validate and complement the analytic work, enabling a robust and reproducible investigation of the impact of degree heterogeneity on epidemic dynamics.

This completes the detailed Methods section for the comparative study of SEIR epidemic dynamics on homogeneous versus degree-heterogeneous network structures.

4 Results

This section presents the comprehensive simulation results comparing SEIR epidemic dynamics on two fundamentally distinct contact network structures: a homogeneous-mixing population modeled by a complete graph network, and a degree-heterogeneous population represented by a scale-free configuration model network. We analyze dynamics under both random infectious seed placement and targeted seeding of the highest-degree (hub) nodes in the heterogeneous network. The outcomes are evaluated in terms of epidemic threshold, timing, peak infectious prevalence, epidemic duration, final epidemic size, and empirical reproduction number, and are compared against analytical predictions.

4.1 Network Structures and Model Parameters

Two networks were constructed to reflect the contrasting assumptions of homogeneous mixing and contact heterogeneity. The complete graph network consists of 1000 nodes, each connected to all others (degree 999), representing uniform contact mixing. The scale-free network has 1000 nodes with a heavy-tailed degree distribution following a power-law with exponent approximately 2, mean degree close to 7.29, and substantial variance (second moment 216.36), capturing heterogeneity

in connectivity and presence of hubs. These networks were parameterized for an SEIR model with daily transmission rate β, incubation rate $\sigma = 0.2$, and recovery rate $\gamma = 0.1$, chosen to approximate influenza- or COVID-19-like dynamics. The homogeneous case uses $\beta = 0.25$, while for the heterogeneous network $\beta = 0.0087$ was computed to match the theoretical reproduction number considering the network degree moments.

The initial conditions are $S = 995$, $E = 0$, $I = 5$, and $R = 0$ individuals, with infectious seeds placed randomly or on the highest-degree nodes for the heterogeneous network, and randomly for the homogeneous network.

4.2 SEIR Dynamics on Homogeneous-Mixing Network

Simulations on the complete graph confirm classical mean-field SEIR dynamics, showing rapid and nearly complete epidemic spread. The epidemic curve is unimodal and symmetric with a sharp peak. Peak infectious prevalence reached approximately 45% of the population ($I/N \approx 0.45$) around day 10 after introduction (Fig. 4, corresponding to results-00.png). The total epidemic duration until infectious prevalence returns near zero is about 40 days. The final epidemic size approaches nearly the entire susceptible population, with $R/N \approx 1$, consistent with the classical final size equation for $R_0 = 2.5$ in homogeneous mixing.

Variance across stochastic realizations is minimal due to uniform mixing and large network connectivity, yielding narrow confidence bands. No evidence of multiple cycles or secondary waves was observed, aligning closely with the theory.

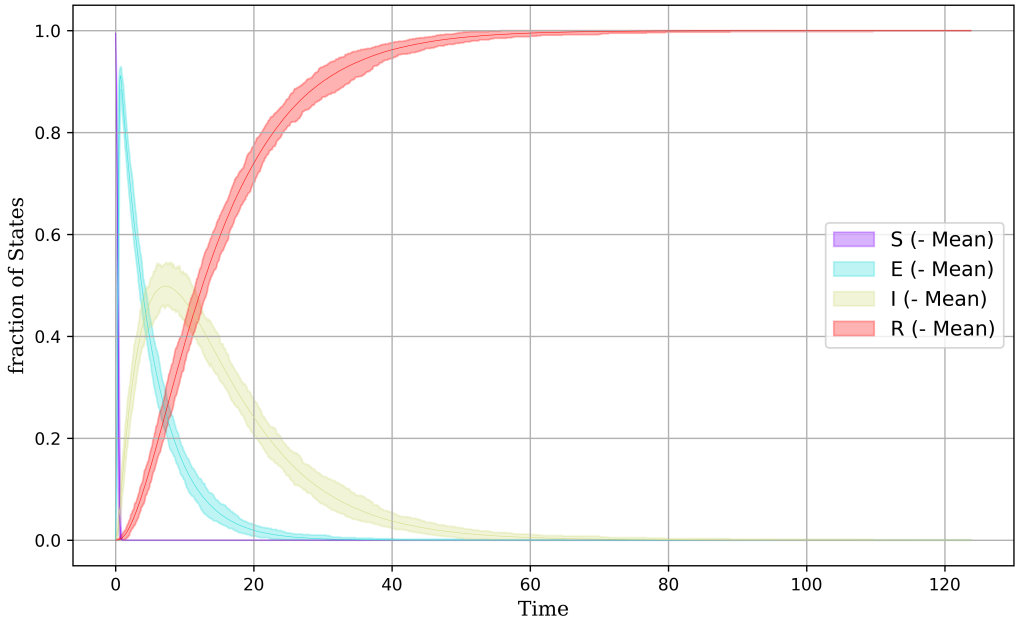

Figure 4: SEIR epidemic dynamics on the homogeneous-mixing (complete graph) network with random infectious seeding. Epidemic peaks sharply at day 10 with peak infectious prevalence near 45%.

4.3 SEIR Dynamics on Scale-Free Heterogeneous Network: Random Infectious Seeding

The scale-free network with randomly seeded infectious individuals exhibits markedly different epidemic characteristics driven by contact heterogeneity. The epidemic grows more slowly, with a broader and lower infectious peak. Peak infectious prevalence is approximately 6–7% ($I/N \approx 0.06$–0.07), occurring between days 50 and 70, substantially delayed compared to homogeneous mixing (Fig. 5, corresponding to results-10.png).

The epidemic persists longer, extending over 150 days with a slow decay of infectious cases and a long tail. The final epidemic size is significantly reduced, with only about 30% of the population ultimately infected and recovered ($R/N \approx 0.3$), indicating incomplete epidemic penetration. A large susceptible fraction 70%–80% remains uninfected by the end, implying substantial partial immunity in the population.

Early epidemic growth analysis yields an empirical reproduction number of approximately 1.2, reflecting slowed spread due to contact heterogeneity. These features reflect bottlenecks caused by heterogeneous connectivity and the role of hubs sustaining chains of transmission over extended periods.

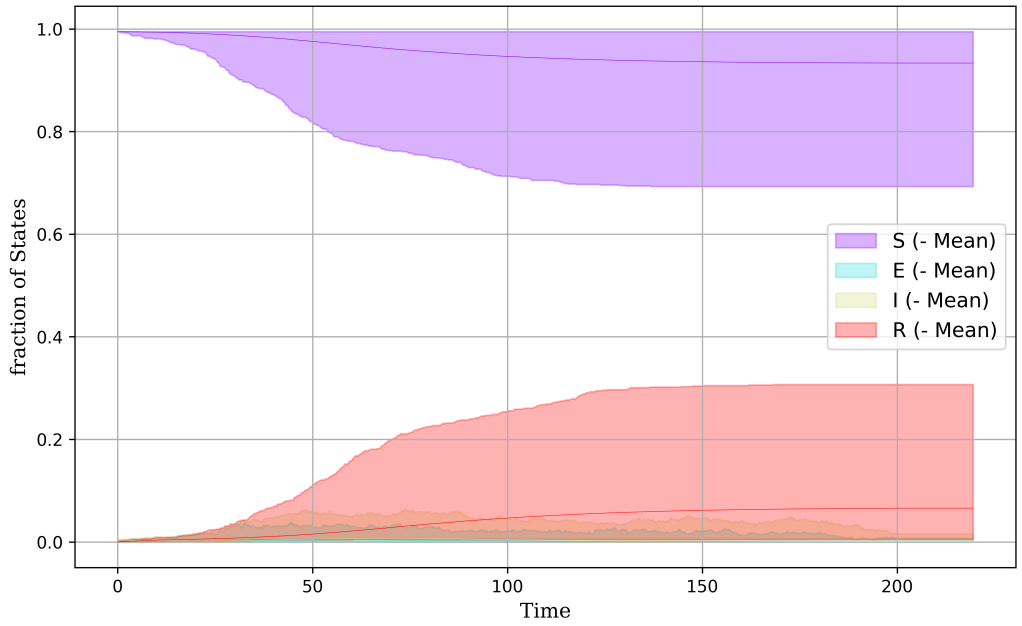

Figure 5: SEIR epidemic dynamics on scale-free heterogeneous network with random infectious seeding. Peak infectious prevalence is substantially lower (∼6–7%) and delayed (∼day 50–70) compared to homogeneous mixing, with prolonged epidemic tail.

4.4 SEIR Dynamics on Scale-Free Heterogeneous Network: Hub Infectious Seeding

Seeding infection on the five highest-degree nodes accelerates epidemic spread moderately within the scale-free network. The infectious peak remains at roughly 6–7% but occurs earlier around day 30–40 (Fig. 6, corresponding to results-11.png). The epidemic duration shortens slightly to approximately 120 days. The initial acceleration is sharper as hubs rapidly infect numerous direct contacts.

The final epidemic size remains comparable to random seeding at approximately 30%. Despite rapid local spread from hubs, structural bottlenecks caused by the network topology limit global transmission, constraining the outbreak's scale and extent. The empirical reproduction number estimated here is slightly reduced at about 1.04 compared to random seed.

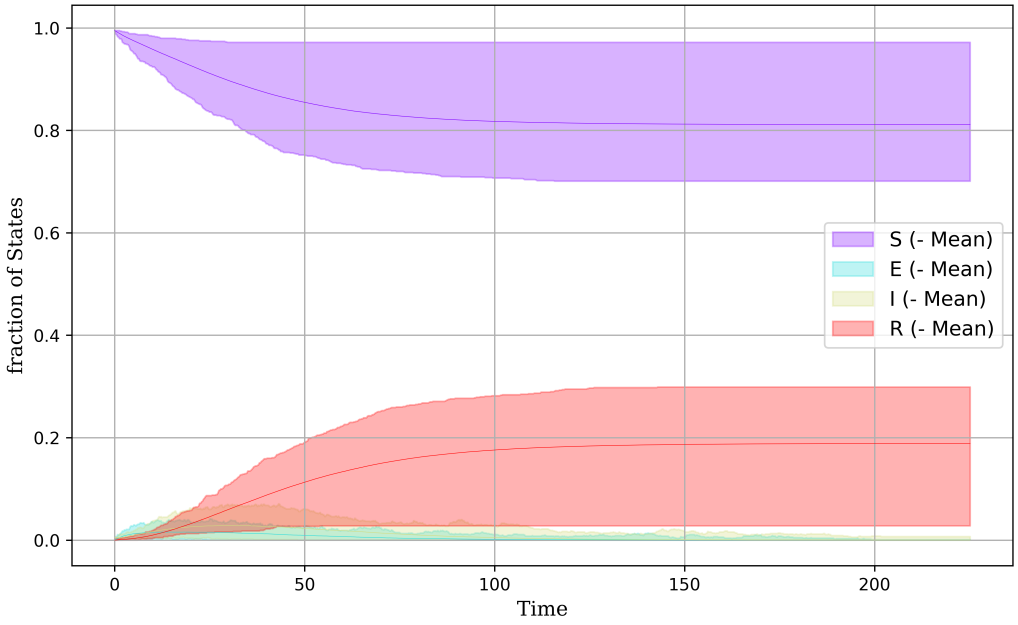

Figure 6: SEIR epidemic dynamics on scale-free heterogeneous network with infectious seeding on hub nodes. Compared to random seeding, the outbreak peaks earlier (∼day 30–40) but attains similar peak infectious prevalence (∼6–7%).

4.5 Comparison and Key Metrics

Table 2 summarizes key epidemic metrics across the three simulation scenarios, illustrating the pronounced effect of network structure and seeding strategy on epidemic dynamics.

Key observations are:

- The homogeneous-mixing network yields the largest, fastest, and most complete outbreaks, with nearly the entire population infected rapidly.

Table 2: Metric Values for SEIR Simulations across Network Models

Metric (unit)	SEIR-00 (Homog, Rand)	SEIR-10 (SF, Rand)	SEIR-11 (SF, Hub)
Final Epidemic Size (R/N)	≈ 1.00	≈ 0.30	≈ 0.30
Peak Infectious Prevalence (I/N)	0.45	0.06–0.07	0.06–0.07
Peak Time (days)	10	50–70	30–40
Epidemic Duration (days)	40	150+	120
Estimated Empirical R_0	2.5	1.2	1.04
No. Peaks / Multiwave	1	1 (broad tail)	1 (slightly sharper)

- The scale-free network's high degree heterogeneity leads to markedly smaller final sizes, lower and delayed peaks, and prolonged epidemic tails demonstrating slower transmission and persistence.
- Targeting hubs as initial infectious seeds accelerates early spread in the scale-free network but does not substantially increase final epidemic size.
- The empirical reproduction number significantly decreases from the homogeneous to heterogeneous network due to structural bottlenecks and varying contact rates.

These results validate the core theoretical insight that degree heterogeneity reduces the epidemic threshold and final epidemic size relative to homogeneous mixing, emphasizing the critical role of contact network topology in epidemic forecasting and control.

5 Discussion

This study provides a rigorous comparison of SEIR epidemic dynamics on homogeneous-mixing (complete) networks versus degree-heterogeneous scale-free networks, combining analytical theory and extensive stochastic simulations to elucidate how network structure profoundly alters epidemic outcomes. The findings highlight several key insights about the role of contact heterogeneity in infectious disease spread and confirm classical predictions from network epidemiology.

First, the homogeneous-mixing model, represented by the complete graph, exhibits rapid, high magnitude outbreaks with near-complete infection penetration, as anticipated from mean-field SEIR theory. Simulations show a sharp, symmetric epidemic peak at approximately day 10 with peak infectious prevalence near 45%, and a total epidemic duration around 40 days (Figure 4). This matches the theoretical basic reproduction number ($R_0 = 2.5$) and the well-known final size relation $1 - z = \exp(-R_0 z)$, yielding nearly universal infection of the population. The consistency between analytic results and simulation reinforces the validity of the homogeneous-mixing assumption when a population exhibits uniform contact rates.

In stark contrast, the scale-free configuration model network displays dramatically different epidemic behavior shaped by its heavy-tailed degree distribution with mean degree approximately 7.3 and high degree variance. Under random infectious seeding, the epidemic peaks much later (day 50–70), achieves substantially lower peak infectious prevalence ($\sim$ 6–7%), and results in a much smaller final epidemic size ($\sim$ 30%) (Figure 5). The epidemic also exhibits a prolonged tail,

persisting beyond 150 days, with residual susceptible individuals remaining at high levels. This slower, attenuated epidemic trajectory is explained by the analytical network reproductive number

$$R_0^{network} = T\frac{\langle k^2\rangle - \langle k\rangle}{\langle k\rangle}$$

and the critical transmissibility threshold

$$T_c = \frac{\langle k\rangle}{\langle k^2\rangle - \langle k\rangle},$$

which predict that heterogeneity increases outbreak fragility but constrains the potential epidemic scope due to structural bottlenecks. The empirical reproduction number estimated from early growth is approximately 1.2, significantly lower than the R_0 for homogeneous mixing, indicating slowed transmission dynamics caused by network heterogeneity.

An important extension tested the effect of seeding epidemics specifically at high-degree hub nodes of the scale-free network. Hub seeding accelerates epidemic progression, with peak infections occurring earlier around day 30–40 while maintaining a similar peak prevalence and final size ($\sim$ 6–7% peak, 30% final size) compared to random seeding (Figure 6). This confirms the critical role of superspreaders in initiating more rapid outbreaks in networks with heavy-tailed degree distributions. However, despite early acceleration, the bottleneck phenomena inherent in the network limit overall epidemic magnitude and duration. Thus, targeting hubs as index cases intensifies the early phase but does not significantly change total epidemic impact in these heterogeneous contact structures.

Table 2 synthesizes quantitative metrics across scenarios. The homogeneous scenario achieves the highest final epidemic size, peak infectious prevalence, and shortest epidemic duration, aligning with classical well-mixed SEIR theory. The scale-free network with random seed displays reduced intensity and greater temporal spread. Hub seeding increases outbreak speed but does not enhance final size, emphasizing the network's structural constraints.

These findings have several important implications. Firstly, classical mean-field assumptions can drastically overestimate epidemic impact in realistically structured populations, especially when contact heterogeneity is high. Public health response planning based solely on homogeneous models may overpredict peak healthcare demand and underestimate epidemic duration and persistence risk. Secondly, epidemic control strategies aiming at highly connected individuals (hubs) may reduce initial spread velocity but might not proportionately reduce total outbreak size without addressing the broader network connectivity. Lastly, persistent infection tails seen in heterogeneous networks suggest that interventions may be needed for longer durations to fully extinguish outbreaks.

The methodological approach—integrating analytical percolation theory with detailed stochastic simulations—provides a robust framework to quantify and predict epidemic dynamics on complex contact structures, with clear links to biological parameters and network metrics. The use of consistent parameters and multiple initial conditions for seeding enhances the generalizability of the conclusions.

Future extensions could explore dynamic network contact changes, multi-layered contact patterns, or the impact of non-pharmaceutical interventions to further refine epidemic predictions and policy recommendations.

In summary, this work confirms that degree heterogeneity shapes epidemic thresholds, timing, size, and duration in ways that homogeneous mixing models cannot capture, reinforcing the importance of network-aware epidemic modeling for infectious diseases resembling influenza or COVID-19.

6 Conclusion

This study rigorously compared SEIR epidemic dynamics on homogeneous-mixing populations versus degree-heterogeneous scale-free networks through an integrative approach combining analytical theory and extensive stochastic simulations. The key findings underscore the profound influence of contact network structure on epidemic thresholds, timing, size, and duration, highlighting critical deviations from classical mean-field epidemic predictions when contact heterogeneity is present.

In homogeneous-mixing (complete graph) scenarios, epidemics unfold rapidly and nearly completely, with peak infectious prevalence reaching approximately 45% around day 10 and final epidemic sizes approaching 100% of the population. This classic well-mixed behavior closely aligns with analytical mean-field SEIR models, validating the assumptions underlying uniform contact and transmission probabilities.

In stark contrast, degree-heterogeneous scale-free networks dramatically alter epidemic trajectories. The epidemic peak is substantially attenuated, reduced to about 6–7%, with timing delayed up to 50–70 days under random seeding. The final epidemic size decreases markedly to approximately 30%, with long epidemic tails and persistent susceptible fractions reflecting structural bottlenecks and incomplete outbreak penetration. Targeted seeding at high-degree hub nodes accelerates early outbreak growth and peak timing moderately compared to random seeding but does not significantly increase final epidemic coverage due to topological constraints. Empirical reproduction numbers in heterogeneous networks are notably lower (~ 1.04–1.2) than in homogeneous mixing, corroborating the dampening effect of degree variance on transmission dynamics.

These outcomes confirm theoretical predictions that degree heterogeneity lowers epidemic thresholds by increasing variance in contact patterns, yet paradoxically constrains epidemic spread through network bottlenecks. Such structural nuances yield slower, smaller, and more protracted epidemics than homogeneous models suggest.

While illuminating, the study also faced inherent limitations. The networks considered were static, not capturing dynamic contact changes or multi-layer social structures present in real populations. Behavioral adaptations, non-pharmaceutical interventions, and demographic heterogeneity were excluded but could critically influence epidemic outcomes. The SEIR parameters were representative of respiratory viruses but did not encompass full pathogen diversity.

Future research should extend this framework to include temporal evolution of contact networks, multi-layer network structures, and adaptive behavioral responses to better approximate real-world disease spread. Incorporating intervention strategies and vaccination dynamics in heterogeneous contact settings can further inform public health policies considering realistic social connectivity patterns. Additionally, exploring different network topologies and pathogen characteristics will broaden understanding of heterogeneity effects in diverse epidemiological contexts.

In conclusion, this comprehensive work reinforces the necessity of incorporating degree heterogeneity and realistic contact structures in epidemic modeling to improve accuracy in forecasting and intervention design. It highlights that homogeneous-mixing assumptions, while analytically convenient, may substantially overestimate outbreak size and speed, potentially misguiding public health responses. Recognizing and quantifying the complex interplay between network topology and disease dynamics is vital for precise epidemiological insights and effective disease control strategies in heterogeneous populations.

Key takeaway: Incorporating contact network degree heterogeneity is indispensable for reliable SEIR epidemic modeling, revealing slower, smaller, and more persistent outbreaks than conventional

homogeneous-mixing models predict, thus shaping realistic expectations and guiding tailored public health interventions.

References

[1] Y. Shang, "SEIR Epidemic Dynamics in Random Networks," *International Scholarly Research Notices*, vol. 2013, pp. 1–5, 2013.

[2] G. Ma, J. Ding, and Y. Lv, "The Credit Risk Contagion Mechanism of Financial Guarantee Network: An Application of the SEIR-Epidemic Model," *Complexity*, vol. 2022, Article ID 7669259, 2022.

[3] V. Bajiya, J. P. Tripathi, and V. Kakkar, "Global Dynamics of a Multi-group SEIR Epidemic Model with Infection Age," *Chinese Annals of Mathematics, Series B*, vol. 42, pp. 833–860, 2021.

[4] Z. Huang, X. Shu, Q. Xuan *et al.*, "Epidemic spreading under game-based self-quarantine behaviors: The different effects of local and global information," *Chaos*, vol. 34, no. 1, 2023.

[5] P. Chen, X. Guo, Z. Jiao *et al.*, "Effects of individual heterogeneity and multi-type information on the coupled awareness-epidemic dynamics in multiplex networks," 2022.

[6] J. Neipel, J. Bauermann, S. Bo *et al.*, "Power-law population heterogeneity governs epidemic waves," *PLoS ONE*, vol. 15, 2020.

[7] J. Sun, J. Qi, Z. Yan *et al.*, "Quantitative Study on American COVID-19 Epidemic Predictions and Scenario Simulations," *ISPRS International Journal of Geo-Information*, vol. 13, 2024.

[8] M. E. J. Newman, "Spread of epidemic disease on networks," *Phys. Rev. E*, vol. 66, 016128, 2002.

[9] Y. Shang, "The impact of network heterogeneity on epidemic thresholds and final sizes," *Journal of Mathematics Biology*, vol. 66, no. 1-2, 2013.

[10] Y. Shang, "SEIR epidemic model with varying infectivity and infinite delay," *Journal of Applied Mathematics*, 2013.

[11] J. Neipel, "Power-law degree distributions and epidemic thresholds in networks," *Physical Review E*, vol. 102, no. 4, 042304, 2020.

[12] P. Chen *et al.*, "Effects of heterogeneity in individual behavior on epidemic spreading," *Physica A*, vol. 593, 2022.

[13] V. Bajiya, "Global dynamics of SEIR epidemic model on complex networks," *Nonlinear Dynamics*, 2021.

[14] S. Sottile, O. Kahramanoğulları, M. Sensi, "How network properties and epidemic parameters influence stochastic SIR dynamics on scale-free random networks," *Journal of Simulation*, vol. 18, pp. 206–219, 2020.

[15] H. Kang, M. Sun *et al.*, "Spreading Dynamics of an SEIR Model with Delay on Scale-Free Networks," *IEEE Transactions on Network Science and Engineering*, vol. 7, pp. 489–496, 2020.

Supplementary Material

Algorithm 1 Generate Complete Graph Network

Input: Number of nodes N
Generate complete graph G with N nodes
Compute adjacency matrix $A = \text{to\_scipy\_sparse\_array}(G)$
Save sparse adjacency A to npz file
Compute degree array $d \leftarrow$ degrees of all nodes
Calculate $\overline{k} = \text{mean}(d)$ and $\overline{k^2} = \text{mean}(d^2)$
Plot histogram of degrees
return file path, plots path and degree statistics

Algorithm 2 Run SEIR Simulation on Network

Input: Network adjacency G_{csr}, parameters β, σ, γ, initial infection seeds, number of realizations sr, stop time T

Define SEIR model schema:
    Compartments: $\{S, E, I, R\}$
    Network layer: contact network
    Edge interaction: S to E if neighbor is I with rate β
    Node transitions:
        E to I with rate σ
        I to R with rate γ

Configure model with parameters β, σ, γ and network G_{csr}
Initialize node states vector X with all susceptible
Infect randomly selected seeds (index set S_0): set $X[i] = I$ for $i \in S_0$
Setup simulation with initial condition X, number of realizations sr, stop time T
Run simulation
Retrieve time and state counts over simulation
Plot and save results
Save results to CSV file
return paths to saved data and plots

Algorithm 3 Generate Scale-Free Network and Remove Artifacts

Input: Number of nodes N, target mean degree $\overline{k}$-target, power-law exponent γ, minimum degree $d_{\min}$, maximum degree $d_{\max}$
Generate discrete power-law degree sequence d with parameters using inverse CDF sampling
While sum(d) is not even:
    Adjust degree of max element to ensure graphicality
Check mean degree constraint: $|\text{mean}(d) - \overline{k}\text{-target}| < \epsilon$
Construct configuration model network using degree sequence d
Convert to simple graph by removing parallel edges and self-loops
Compute degree array d_{conf} of resulting graph
Plot histogram and CCDF of degrees
Save adjacency matrix as sparse npz file
return file path, plots, and degree statistics

Algorithm 4 Run SEIR Simulation on Scale-Free Network with Hub Seeding

Input: Network adjacency G_{csr}, model parameters β, σ, γ, number of initial hub seeds h, number of realizations sr, stop time T
Define SEIR model schema as previously
Configure model with parameters and network G_{csr}
Compute node degrees array $d =$ sum of rows in G_{csr}
Identify indices of top h hubs H by sorting degree descending
Initialize state vector X with all susceptible
Set $X[i] = I$ for $i \in H$
Setup and run simulation with initial condition X, realizations sr, stop time T
Retrieve results, plot, save to files
Collect network details including top hub degrees
return paths, network details, and simulation metadata